

Layered Lithium Iron Nitride: A Promising Anode Material for Li-Ion Batteries

Jesse L. C. Rowsell, Valérie Pralong, and Linda F. Nazar*

University of Waterloo, Department of Chemistry
Waterloo, Ontario, Canada N2L 3G1

Received May 24, 2001

Rechargeable lithium-ion cells are currently considered the most promising energy storage systems. The process in the cell involves simultaneous intercalation–deintercalation of Li ions in two electrode host materials, one at low potential (anode) and one at high potential (cathode). The commercial cell is composed of a carbon-based anode, a layered transition metal oxide as the cathode, and a nonaqueous electrolyte.¹ The limited gravimetric capacity (<370 mA·h/g) of carbon, however, has prompted an intensive search for alternative materials that can intercalate lithium ions at low potential.² Among the few candidates under consideration, lithiated transition metal nitrides have recently emerged as one of the most promising.³ The first studied was LiMoN_2 ,⁴ but the material capturing current interest is $\text{Li}_{2.6}\text{Co}_{0.4}\text{N}$, which exhibits reversible capacity between 480 and 760 mA·h/g.⁵ Cells utilizing it as an anode material are currently under exploratory development.⁶ Its layered morphology is advantageous, supporting fast Li-ion conduction and low transition metal oxidation states.⁷ There are few other reported nitrides that display excellent behavior at low potential; even the Ni and Cu members of the $\text{Li}_2(\text{Li}_{1-x}\text{M}_x)\text{N}$ series have been shown to be inferior.^{5b} An ideal material, however, would be based on Fe or Mn, owing to the high cost and toxicity of cobalt compounds, but their preparation is difficult. Here we report the synthesis and electrochemical performance of the new Fe compound, $\text{Li}_{2.7}\text{Fe}_{0.3}\text{N}$. Its reversible capacity (550 mA·h/g) compares well with that of $\text{Li}_{2.6}\text{Co}_{0.4}\text{N}$, and preliminary results indicate good rate capability over repeated cycling.

The structures exhibited by the Li–M–N (M = first-row transition metal) system follow a predictable trend. For Ti through Fe, an antifluorite structure is favored with Li and M in the tetrahedral sites; M being present in a high oxidation state.⁸ For Co, Ni, and Cu, a structure based on $\alpha\text{-Li}_3\text{N}$ is formed, with M^+ substituting for lithium between the hexagonal Li_2N layers. Iron is unique in forming a “metastable” layered phase Li_4FeN_2 which displays ordering of Fe^{2+} with vacancies between the layers (Figure 1).⁹ Recently, crystals of $\text{Li}_2(\text{Li}_{0.37}\text{Fe}_{0.67})\text{N}$ have been isolated from a mixture formed from decomposition of the antifluorite phase in a lithium flux.¹⁰

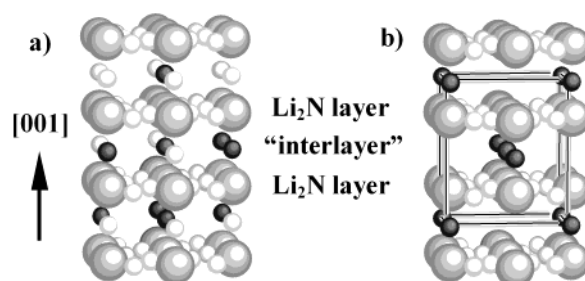


Figure 1. Structures of (a) $\text{Li}_2(\text{Li}_{1-x}\text{Fe}_x)\text{N}$ (space group $P6/mmm$) and (b) Li_4FeN_2 , or “ $\text{Li}_2(\square_{0.5}\text{Fe}_{0.5})\text{N}$ ” (space group $Immm$), with unit cell outlined. Nitrogen atoms are drawn as large spheres, and lithium as small pale spheres.

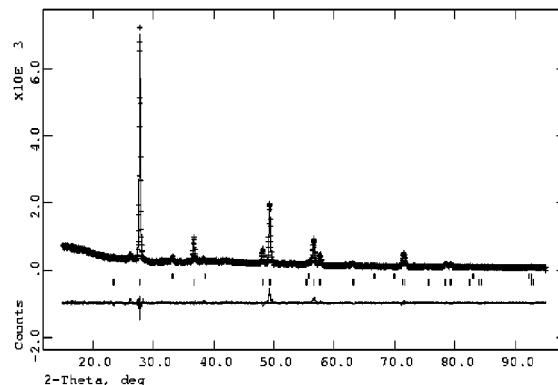


Figure 2. Powder XRD pattern of $\text{Li}_{2.7}\text{Fe}_{0.3}\text{N}$. Observed data are indicated by (+) marks, and the calculated pattern and difference curves are shown with solid lines. The top row of tick marks indicates positions of Li_2O reflections, while the bottom row are those calculated for $\text{Li}_{2.7}\text{Fe}_{0.3}\text{N}$.

We devised a novel synthesis route to the layered $\text{Li}_2(\text{Li}_{0.7}\text{Fe}_{0.3})\text{N}$ compound that provides a higher (100%) yield in a much shorter time than the Li flux method. The process is simple and is capable of providing gram-scale quantities within 1 day.¹¹ Powder X-ray diffraction (XRD) of the products shows that the composition is virtually independent of firing temperature. As the melt is in contact with an excess source of iron, it reaches a “saturation point” in a process that parallels dissolution. The level of substitution $x = 0.3$ was determined by Rietveld refinement of the powder XRD pattern (Figure 2).^{12,13}

While a thermal quenching technique was previously used to isolate the ordered $\text{Li}_2(\square_{0.5}\text{Fe}_{0.5})\text{N}$ crystals from a mixture, only the disordered $\text{Li}_2(\text{Li}_{0.7}\text{Fe}_{0.3})\text{N}$ compound is obtained using the synthesis reported here. As observed for the other $\text{Li}_2(\text{Li}_{1-x}\text{M}_x)\text{N}$ compounds, there is an expansion in the a unit cell parameter and a contraction in c as x increases. Our values form a linear

(1) (a) Thackeray, M. M.; Thomas, J. O.; Whittingham, M. S. *MRS Bull.* **2000**, 25, 39. (b) Nazar, L. F.; Goward, G. R.; Duncan, M. J.; Leroux, F.; Huang, H. J. *Int. Inorg. Mater.* **2001**, 3, 191.

(2) (a) Goward, G. R.; Nazar, L. F.; Power, W. P. *J. Mater. Chem.* **2000**, 10, 1241. (b) Vaughey, J. T.; O'Hara, J.; Thackeray, M. M. *Electrochem. Solid-State Lett.* **2000**, 3, 13.

(3) Hasegawa, M.; Yamaura, J.; Tsutsumi, S.; Nitta, Y.; Shodai, T.; Sakurai, Y. 1999 Joint Int. Meeting, Hawaii, 1999, Abstract 174.

(4) Elder, S. H.; Doerrer, L. H.; DiSalvo, F. J.; Parise, J. B.; Guyomard, D.; Tarascon, J. M. *Chem. Mater.* **1992**, 4, 928.

(5) (a) Nishijima, M.; Kagohashi, T.; Imanishi, M.; Takeda, Y.; Yamamoto, O.; Kondo, S. *Solid State Ionics* **1996**, 83, 107. (b) Shodai, T.; Okada, S.; Tobishima, S.; Yamaki, J. *Sol. State Ionics* **1996**, 86–88, 785.

(6) Nitta, Y.; Yamaura, J.; Hasegawa, M.; Tsutsumi, S.; Ohzono, H.; Miyake, H. 10th International Meeting on Lithium Batteries, Como, Italy, May, 28–June 2, 2000, Abstract 71.

(7) Sachsze, W.; Juz, R. Z. *Anorg. Allg. Chem.* **1948**, 259, 278.

(8) Juz, R.; Langer, K.; von Benda, K. *Angew. Chem., Int. Ed. Engl.* **1968**, 7, 360.

(9) Gudat, A.; Kniep, R.; Rabenau, A. *Angew. Chem., Int. Ed. Engl.* **1991**, 30, 199.

(10) Klatyk, J.; Kniep, R. Z. *Kristallogr.* **1999**, 214, 447.

(11) Pressed chunks of Li_3N (Alfa Aesar, 99.5%) were fused in a pure iron vessel (Goodfellow, 99.5%) that was sealed under 300 kPa of nitrogen. The product could be formed in the temperature range 850–1050 °C, roughly defined by the liquid range of Li_3N . Reactions were fired for 12 h before thermally quenching the vessel. The air-sensitive compounds were manipulated within an argon glovebox.

(12) The black crystalline powder was ground and sealed within an airtight hemicylindrical cell under argon. Data were collected in Bragg–Brentano geometry on a Siemens D-500 diffractometer equipped with a diffracted beam monochromator (Cu K α radiation) in the range $15^\circ < 2\theta < 95^\circ$. The structure was refined using GSAS software.¹³ $\text{Li}_{2-x}\text{Fe}_x\text{N}$, $x = 0.29(1)$ in space group $P6/mmm$ (no. 191) with $a = 3.6853(6)$ Å, $c = 3.7677(6)$ Å, $V = 44.32(2)$ Å³, $Z = 1$, $\rho_{\text{calc}} = 1.836(2)$ g cm⁻³. Atoms were placed on the special positions observed for the other $\text{Li}_2(\text{Li}_{1-x}\text{M}_x)\text{N}$ compounds,⁷ and the Fe/Li ratio was refined on the Li(1) site by assuming no vacancies. Lithium oxide was modeled as a secondary phase, and amounted to 2% of the sample. The refinement converged with $R_p = 0.070$, $wR_p = 0.094$.

(13) Larson, A. C.; Von Dreele, R. B. *General Structure Analysis System (GSAS)*; Los Alamos National Laboratory Report LAUR 86-748 2000.

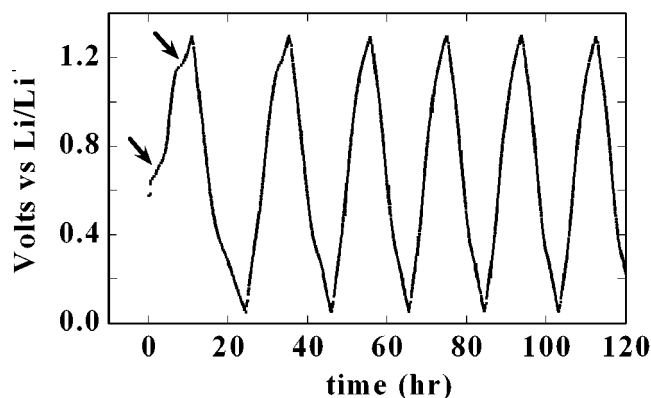


Figure 3. Galvanostatic charge/discharge of $\text{Li}_{2.7}\text{Fe}_{0.3}\text{N}$ at C/10 in the potential window 0.05–1.3 V. Arrows indicate the two two-phase transitions discussed in the text.

relationship with those of the end members ($x = 0^{14}$ and $x = 0.63^{10}$), as expected for solid solutions.

Interest in layered lithium iron nitride arises from the fact that Li^+ ions may be intercalated and extracted reversibly over a wide range of Li composition at low potential. The electrochemical properties of $\text{Li}_{2.7}\text{Fe}_{0.3}\text{N}$ were investigated using standard cells with a metallic lithium counter-electrode serving as the Li-ion source.¹⁵ Unlike the isostructural Ni and Cu compounds, the material shows high specific capacity, even when cycled at current densities of $0.16 \text{ mA}\cdot\text{cm}^{-2}$ (equivalent to C/10 for one Li). The potential curve of the charge–discharge–charge sequence is shown in Figure 3. Up to 1.1 Li per formula unit can be extracted on initial charging to 1.3 V, which occurs in two separate steps, indicating two transitions. Curiously, this is different from the layered cobalt compound, which only exhibits a single plateau at $\sim 1 \text{ V}$.^{5b}

The formation of an amorphous compound for $\text{Li}_{2.6}\text{Co}_{0.4}\text{N}$ on electrochemical oxidation is thought to be critical to its performance. Ex situ powder XRD studies show that $\text{Li}_{2.7}\text{Fe}_{0.3}\text{N}$ also transforms to an amorphous material after one charge–discharge cycle, but by a more complex route. Figure 4 illustrates the changes that occur. After extraction of 0.5 Li, the reflections of the starting phase disappear and are replaced by a very broad feature spanning the region $15^\circ < 2\theta < 30^\circ$ (Figure 4b). This reflection has a maximum in intensity similar in d spacing to the (001) reflection of the $\text{Li}_2(\text{Li}_{1-x}\text{M}_x)\text{N}$ structure at 3.9 Å, but almost zero intensity in $\text{Li}_{2.7}\text{Fe}_{0.3}\text{N}$. Upon charging to 1.3 V (extraction

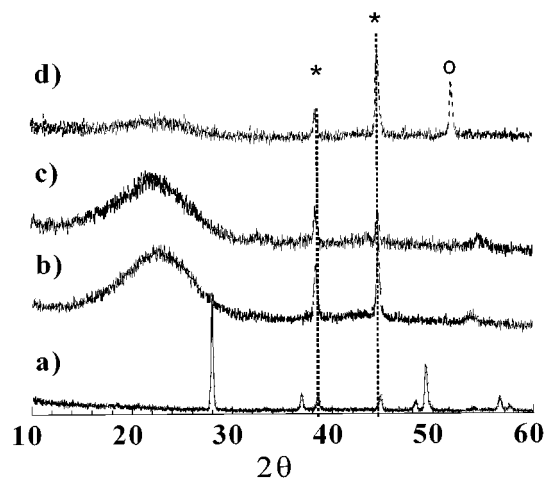


Figure 4. Ex situ powder XRD patterns of $\text{Li}_{2.7}\text{Fe}_{0.3}\text{N}$ on charge–discharge: (a) starting material, (b) after extraction of 0.5 Li, (c) after extraction of 1.1 Li, (d) after discharge to 0.05 V. Reflections due to the aluminum sample holder and the nickel current collector are marked by asterisks and circles, respectively.

of 1.1 Li), the broad feature is retained. That the first step corresponding to the formal partial oxidation of Fe^{1+} is an order–disorder transition is suggested by the appearance of the broad peak. It is likely the lithium is first extracted from between the Li_2N layers on this first step and then from within them, resulting in structural collapse in two stages. The first extraction of 0.5 Li would leave the interlayer region void of lithium, in a highly disordered, iron-deficient variant of $\text{Li}_2(\square_{0.5}\text{Fe}_{0.5})\text{N}$ (Figure 1b). Further extraction of 0.6 Li from the Li_2N layer may leave some interlayer structural coherence, evidenced by the broad reflection in Figure 4c.

More lithium can be inserted in the quasi-amorphous material on the following discharge (1.3 Li) than was extracted on charge, yielding an amorphous material (Figure 4d). On the following charge sweep, 1.04 Li can be extracted, giving a reversible capacity of $550 \text{ mA}\cdot\text{h/g}$. Together with the attractive average redox potential of 0.6 V versus Li/Li^+ , these properties demonstrate that this compound is both chemically intriguing and potentially attractive as an anode material for rechargeable lithium-ion batteries. Current work is focused on optimizing this material and obtaining a precise understanding of the Li (de)insertion mechanism for this class of compounds.

Acknowledgment. We gratefully acknowledge the NSERC for financial support through their Research, Strategic, and Scholarship programs.

JA0112745

(14) Rabenau, A.; Schulz, H. *J. Less-Common Met.* **1976**, *50*, 155.

(15) Swagelok cells were constructed using 1 M LiPF_6 in EC-DMC (Merck) as the electrolyte, as described elsewhere.^{2a} The working electrode was fabricated from 25% acetylene black, and 75% active material, pressed onto a nickel disk. Galvanostatic cycling was performed using a MacPile controller (Biologic, Claix, France). Cells contained $\sim 6 \text{ mg}$ of active material in an electrode surface area 1.1 cm^2 .